NeuroImage: Clinical 5 (2014) 408–419

Contents lists available at ScienceDirect

NeuroImage: Clinical

journal homepage: www.elsevier.com/locate/ynicl

Voxel-wise resting-state MEG source magnitude imaging study reveals neurocircuitry abnormality in active-duty service members and veterans with PTSD

Ming-Xiong Huang[a,b,*], Kate A. Yurgil[a,c], Ashley Robb[a], Annemarie Angeles[a], Mithun Diwakar[b], Victoria B. Risbrough[a,c,d], Sharon L. Nichols[e], Robert McLay[f], Rebecca J. Theilmann[b], Tao Song[b], Charles W. Huang[g], Roland R. Lee[a,b], Dewleen G. Baker[a,c,d]

[a] Radiology, Research, and Psychiatry Services, VA San Diego Healthcare System, San Diego, CA, USA
[b] Department of Radiology, University of California San Diego, San Diego, CA, USA
[c] VA Center of Excellence for Stress and Mental Health, San Diego, CA, USA
[d] Department of Psychiatry, University of California San Diego, San Diego, CA, USA
[e] Department of Neurosciences, University of California San Diego, San Diego, CA, USA
[f] Naval Medical Center San Diego, San Diego, CA, USA
[g] Department of Bioengineering, University of California San Diego, San Diego, CA, USA

ARTICLE INFO

Article history:
Received 28 May 2014
Received in revised form 25 July 2014
Accepted 2 August 2014
Available online 7 August 2014

Keywords:
MEG
Post-traumatic stress disorder
Amygdala
Ventromedial prefrontal cortex
Orbitofrontal cortex
Precuneous

ABSTRACT

Post-traumatic stress disorder (PTSD) is a leading cause of sustained impairment, distress, and poor quality of life in military personnel, veterans, and civilians. Indirect functional neuroimaging studies using PET or fMRI with fear-related stimuli support a PTSD neurocircuitry model that includes amygdala, hippocampus, and ventromedial prefrontal cortex (vmPFC). However, it is not clear if this model can fully account for PTSD abnormalities detected directly by electromagnetic-based source imaging techniques in resting-state. The present study examined resting-state magnetoencephalography (MEG) signals in 25 active-duty service members and veterans with PTSD and 30 healthy volunteers. In contrast to the healthy volunteers, individuals with PTSD showed: 1) hyperactivity from amygdala, hippocampus, posterolateral orbitofrontal cortex (OFC), dorsomedial prefrontal cortex (dmPFC), and insular cortex in high-frequency (i.e., beta, gamma, and high-gamma) bands; 2) hypoactivity from vmPFC, Frontal Pole (FP), and dorsolateral prefrontal cortex (dlPFC) in high-frequency bands; 3) extensive hypoactivity from dlPFC, FP, anterior temporal lobes, precuneous cortex, and sensorimotor cortex in alpha and low-frequency bands; and 4) in individuals with PTSD, MEG activity in the left amygdala and posterolateral OFC correlated positively with PTSD symptom scores, whereas MEG activity in vmPFC and precuneous correlated negatively with symptom score. The present study showed that MEG source imaging technique revealed new abnormalities in the resting-state electromagnetic signals from the PTSD neurocircuitry. Particularly, posterolateral OFC and precuneous may play important roles in the PTSD neurocircuitry model.

1. Introduction

Individuals exposed to a traumatic event may develop post-traumatic stress disorder (PTSD) with debilitating post-traumatic stress symptoms, including intrusive memories, avoidance behavior, emotional numbing, and hyperarousal (American Psychiatric Association, 2004). PTSD is a major health concern that affects approximately 7.7% of Americans (Kessler et al., 1995, 2005) and is particularly prevalent among military service members who have served in combat (Dohrenwend et al., 2006; Magruder and Yeager, 2009). The recent conflicts in Iraq and Afghanistan have been no exception, with combat veterans returning with elevated rates of PTSD (Hoge et al., 2004; Smith et al., 2008; Tanielian and Jaycox, 2008).

In light of these findings, much effort has been focused on determining symptom etiology and the associated neural mechanisms of PTSD. The development of neurocircuitry models of PTSD has relied strongly on findings from pre-clinical studies of fear conditioning. Evidence from lesion studies, pharmacological manipulations, and electrophysiology in animals and humans suggest that interactions between the amygdala, ventromedial prefrontal cortex (vmPFC), and hippocampus control different aspects of fear processing (Hartley and Phelps, 2010; Rosen and Lilienfeld, 2008). The amygdala is involved in acquisition of

* Corresponding author at: Radiology Imaging Laboratory, University of California at San Diego, 3510 Dunhill Street, San Diego, CA 92121, USA.
E-mail address: mxhuang@ucsd.edu (M.-X. Huang).

http://dx.doi.org/10.1016/j.nicl.2014.08.004

fear conditioning and extinction learning, whereas the vmPFC is thought to mediate memory storage and retrieval during extinction learning. Hippocampal connections to the amygdala and vmPFC may support processing contextual information of threat-related stimuli.

Amygdala, vmPFC, and hippocampal regions implicated in preclinical fear processing are thought to be dysfunctional in PTSD (Rauch et al., 1998, 2006). Functional neuroimaging findings using positron emission topography (PET) and functional magnetic resonance imaging (fMRI) suggest that individuals with PTSD exhibit hyperresponsive amygdala activity to trauma or fear-related stimuli (Shin and Liberzon, 2010), during emotionally neutral tasks (Bryant et al., 2005; Shin et al., 2004b), and even at rest (Chung et al., 2006; Semple et al., 2000). A hyperresponsive amygdala contributes to the exaggerated fear response characteristic of PTSD (Anderson et al., 2003). Conversely, PTSD has been associated with a hyporesponsive vmPFC (Hughes and Shin, 2011). A hyporesponsive PFC, as well as reduced connectivity to the amygdala (Jin et al., 2013; Shin et al., 2004a) may indicate insufficient inhibitory control over exaggerated fear responses. Lastly, abnormal hippocampal function (Corcoran and Maren, 2001) and reduced connectivity to the amygdala (Dolcos et al., 2004; McGaugh, 2004) may be associated impairments in contextual memory processing and the ability to inhibit intrusive memories (Shin et al., 2004a), although findings have been mixed (Hughes and Shin, 2011). A recent resting-state fMRI study showed increased activity in amygdala and reduced spontaneous neural activity in the dlPFC, but no abnormal decrease of resting-state fMRI activity in the vmPFC (Yan et al., 2013).

Neuroimaging studies using PET and fMRI have contributed greatly to understanding PTSD neurocircuitry in humans; however, these techniques measure metabolic and hemodynamic changes which reflect neuronal activity indirectly (Logothetis, 2003). In addition, PET and fMRI techniques have limited temporal resolution (minutes to seconds) and consequently limited coverage and resolution in the frequency domain. Since neurons communicate to each other via exchanging electric current signals, direct electrophysiological measures are required to study neurophysiological processes that are associated with these hemodynamic signals (Scholvinck et al., 2013). PET and fMRI studies also have implicated different neural pathways that may be hyporesponsive in PTSD; thus, there is some remaining discrepancy whether PTSD is associated with reduced activity in the vmPFC or dlPFC pathways. Furthermore, although the orbitofrontal cortex (OFC) is usually considered to be part of the extended limbic system, the contribution of OFC to PTSD has not been fully elucidated.

Electromagnetic measures such as magnetoencephalography (MEG) provide direct measurements of neuronal activity with millisecond temporal resolution. Using a single dipole model, Kolassa and colleagues reported elevated production of focally generated slow waves (1–4 Hz) in PTSD, particularly in left temporal brain regions, with peak activities in the region of the insula. Using a MEG sensor-space synchronous neural interactions analysis, Georgopoulos, Engdahl, and their colleagues correctly classified individuals with PTSD and healthy control subjects with >90% overall accuracy of classification (Georgopoulos et al., 2010). They also found differences in MEG communication measures between temporal and parietal and/or parieto-occipital right hemispheric areas with other brain areas in PTSD (Engdahl et al., 2010). However in sensor space, it is difficult to determine whether the structures identified by PET and fMRI in PTSD neurocircuitry generate abnormal electromagnetic activity. Namely, whether electromagnetic-based source imaging techniques will lead to similar or different findings from those obtained in PET and fMRI in PTSD neurocircuitry has largely been unexplored.

In the current study, we examined neural activity associated with PTSD using resting-state MEG. MEG is a non-invasive functional imaging technique that directly measures magnetic signals generated by neuronal current in gray matter with high temporal resolution (<1 ms) and spatial localization accuracy (2–3 mm at cortical level) (Leahy et al., 1998). MEG's high temporal resolution directly translates into a wide range of coverage for the neuronal magnetic signals in the frequency domain, which is usually divided into different frequency bands. MEG's insensitivity to the electric conductivity profile of the head tissue makes it a better technique than electroencephalography (EEG) in localizing neuronal sources. Our newly developed high-resolution MEG source imaging method called Fast-VESTAL allowed us to perform voxel-wise whole-brain source imaging of human brain rhythms in healthy volunteers (Huang et al., 2014a), and makes MEG source imaging a good candidate for localizing abnormal electromagnetic signals in disorders such as PTSD. The primary goal for this study was to examine if the existing PTSD neurocircuitry model including the amygdala, vmPFC, and hippocampus can account for abnormalities detected directly by electromagnetic-based source imaging techniques in resting-state. To achieve this goal, we used high-resolution MEG source imaging technique for direct examination of neuronal activity in PTSD, especially in the areas that we think to be abnormal, i.e. amygdala, vmPFC, OFC, hippocampus, dlPFC, dmPFC including dorsal anterior cingulate cortex (dACC), insular cortex, and precuneous. In addition, using MEG, we are able to explore potential MEG abnormalities in different frequency bands which are associated with different neuronal mechanisms (see Discussion), and compare MEG findings with previously published results from other functional imaging techniques that have been used to study PTSD.

2. Materials and methods

2.1. Research participants

Twenty-five participants (24 males, 1 female; mean [SD] age: 31.0 [5.5]) with PTSD took part in this study. Among these participants, 10 were active-duty Marines and Sailors from Camp Pendleton and Naval Medical Center in San Diego, and 15 were adult outpatient OEF/OIF Veterans recruited from VA San Diego Healthcare System. Mean [SD] years of education for the participants with PTSD were 13.2 [1.4]. All participants gave written informed consent for study procedures, which were reviewed and approved by institutional review boards of the VA San Diego Healthcare System and Naval Health Research Center at San Diego. The informed consent followed the ethical guidelines of the Declarations of Helsinki (1975) and additional research requirements for active-duty military personnel and veterans.

Symptoms of PTSD were assessed using the Clinician Administered PTSD Scale (CAPS) (Blake et al., 1995) or the Post-traumatic Stress Disorder Checklist (PCL) (Weathers et al., 1999) in accordance with the criteria from the Diagnostic and Statistical Manual of Mental Disorders IV-TR (American Psychiatric Association, 2000). A total of 18 participants met the criteria for PTSD and 7 met the criteria for partial PTSD. Participants who completed the CAPS met the criteria for PTSD ($n = 14$) if they reported at least 1 re-experiencing symptom, 3 avoidance symptoms, and 2 hyperarousal symptoms; patients met the criteria for partial PTSD ($n = 5$) if they reported at least 1 re-experiencing symptom and either 3 avoidance symptoms or 2 hyperarousal symptoms (Blanchard et al., 1995). Symptoms must have occurred at least once within the past month (frequency ≥ 1) and have caused a moderate amount of distress (intensity ≥ 2) (Weathers et al., 1999, 2001). Participants who completed the PCL questionnaire and had a minimum total score of 50 met the criteria for PTSD ($n = 3$), and those with scores from 39 to 49 met the criteria for partial PTSD ($n = 2$) (Hoge et al., 2008; Iversen et al., 2008; Renshaw, 2011; Weathers et al., 1993). Study participants with partial PTSD and PTSD were analyzed together ($n = 25$) to maintain statistical power and to examine broad group differences in PTSD neurocircuitry. The PTSD patients were not on medications at the time of the MEG exam. All had discontinued any psychotropic medications prior to the scan, and at least at 5-day wash-out.

We recruited thirty healthy volunteers (29 male, 1 female; mean [SD] age: 29.8 [6.4]) with no history of neurological or psychiatric disorders assessed by Structured Clinical Interview for DSM-IV. Among these healthy volunteers, 12 were active-duty military personnel and 18 were

civilians. Mean [SD] years of education were 13.4 [1.7]. There were no statistically significant differences in age or education between the healthy volunteer and PTSD groups.

Exclusion criteria for study participation were as follows: 1) other neurological, developmental or psychiatric disorders (e.g., brain tumor, stroke, epilepsy, Alzheimer's disease, or schizophrenia, bipolar disorder, history of learning disability, or lesions visible in structural MRI); 2) substance or alcohol abuse according to DSM-IV criteria within the 6 months prior to the study; 3) history of metabolic or other diseases known to affect the central nervous system (Dikmen et al., 1995); and 4) extensive metal dental hardware (e.g., braces and large metal dentures; fillings are permitted) or other metal objects in the head, neck, or face areas that cause non-removable MEG artifacts.

2.2. MEG data acquisition and signal pre-processing to remove artifacts

Resting-state MEG data (spontaneous recording for detecting MEG slow-wave signals) were collected at the UCSD MEG Center using the VectorView™ whole-head MEG system (Elekta-Neuromag, Helsinki, Finland) with 306 MEG channels. Participants sat inside a multi-layer magnetically-shielded room (IMEDCO-AG) (Cohen et al., 2002). Precautions were taken to ensure head stability; foam wedges were inserted between the participant's head and the inside of the unit, and a Velcro strap was placed under the participant's chin and anchored in superior and posterior axes. Head movement across different sessions was about 2–3 mm. MEG recording was divided into two 5-minute blocks with eyes closed, alternating with two 5-minute blocks with eyes open. In the eyes-closed condition, the participant was instructed to keep his/her eyes closed and empty his/her mind. In the eyes-open condition, the participant was instructed to fix his/her eyes on a fixation point and empty his/her mind. The order of blocks was counter-balanced between participants. Data were sampled at 1000 Hz and were run through a high-pass filter with a 0.1 Hz cut-off, and a low-pass filter with a 300 Hz cut-off. The filter associated with MEG data acquisition is a first-order time-domain filter with 3 dB around the cut-off points. Eye blinks, eye movements, and heart signals were monitored. Since the MEG eyes-open data were contaminated with eye-blinks in many participants, we focused on analyzing the eyes-closed data in the present study.

Substantial efforts were taken to help ensure that participants were alert during the MEG recordings. Participants were scheduled early in the day to avoid fatigue from performing daily activities. Prior to all of the study sessions, participants completed a questionnaire about the number of hours they slept the previous night, how rested they felt, and if there was any reason that they might not be attentive and perform to the best of their abilities (due to headache, pain, etc.). Sessions alternated between eyes-closed and eyes-open conditions, and eye blinking and movement were monitored. During MEG recording, participants were viewed on camera while technicians also monitored alpha band oscillations, which are consistently associated with tonic alertness (Oken et al., 2006).

Eyes-closed MEG data were first run through MaxFilter, also known as signal space separation (Song et al., 2008; Taulu et al., 2004a,b) to remove external sources of interference (e.g., magnetic artifacts due to metal objects, strong cardiac signals, environment noises), and to co-register the MEG data by removing the small head movements across the two 5-minute eyes-closed sessions. Next, residual artifacts due to eye movements and residual cardiac signals were removed using Independent Component Analysis using our customized version of ICALAB software (www.bsp.brain.riken.jp/ICALAB/).

2.3. Structural MRI, MEG-MRI registration, BEM forward calculation

Structural MRI of the participant's head was collected using a General Electric 1.5 T Excite MRI scanner. The acquisition contains a standard high-resolution anatomical volume with a resolution of $0.94 \times 0.94 \times 1.2\ mm^3$ using a T1-weighted 3D-IR-FSPGR pulse sequence. To co-register the MEG with MRI coordinate systems, three anatomical landmarks (i.e., left and right pre-auricular points, and nasion) were measured for each participant using the Probe Position Identification system (Polhemus, USA). By using MRILAB (Elekta/Neuromag) to identify the same three points on the participant's MR images, a transformation matrix involving both rotation and translation between the MEG and MR coordinate systems was generated. To increase the reliability of the MEG–MR co-registration, approximately 80 points on the scalp were digitized with the Polhemus system, in addition to the three landmarks, and those points were co-registered onto the scalp surface of the MR images. The T1-weighted images were also used to extract the brain volume and innermost skull surface (SEGLAB software developed by Elekta/Neuromag). Realistic Boundary Element Method (BEM) head model was used for MEG forward calculation (Huang et al., 2007; Mosher et al., 1999). The BEM mesh was constructed by tessellating the inner skull surface from the T1-weighted MRI into ~6000 triangular elements with ~5 mm size. A cubic source grid with 5 mm size was used for calculating the MEG gain (i.e., lead-field) matrix, which leads to a grid with ~10,000 nodes covering the whole brain. Other conventional MRI sequences typical for identifying structural lesions were also performed: 1) Axial T2*-weighted; 2) Axial fast spin-echo T2-weighted; and 3) Axial FLAIR. These conventional MRIs were carefully reviewed by a Board-certified neuroradiologist (R.R. Lee) to determine if the participant had visible lesions on MRI. Subjects with lesions visible in MRI were excluded from the study (see exclusion criteria).

2.4. MEG slow-wave source magnitude imaging using fast-VESTAL

The voxel-wise MEG source magnitude images were obtained using our recent high-resolution Fast-VESTAL MEG source imaging method (Huang et al., 2014a). This approach requires the sensor waveform covariance matrix. Here, the second 5-minute resting-state MEG sensor-waveform dataset was registered to the first 5-minute resting-state dataset using MaxFilter. The artifact-free, eyes-closed, resting-state MEG sensor-waveform datasets were divided into 2.5 s epochs. The data in each epoch were first DC-corrected and then run through band-pass filters for the following frequency bands: alpha band (8–12 Hz), beta band (15–30 Hz), gamma band (30–80 Hz), high-gamma band (80–150 Hz), and low-frequency band (1–7 Hz) that combined delta (1–4 Hz) and theta bands (4–7 Hz). Notch filters at 60 Hz and 120 Hz were applied to remove the power line signals and their second harmonics. Frequency-domain band-pass filter with zero phase-shift via discrete Fourier transform was used. At each end of the band-pass filter, the transition of the Hanning window in the filter was selected to be at 10% of the associated cut-off frequency.

Waveforms from all 306 sensors including 204 planar-gradiometers and 102 magnetometers were used in the analysis. For each frequency band, sensor-waveform covariance matrices were calculated for individual epochs after the band-pass filtering, then, the final sensor-waveform covariance matrix was obtained by averaging the covariance matrices across individual epochs for the 10-minute resting-state data. Using such a covariance matrix, MEG slow-wave source magnitude images that cover the whole brain were obtained for each participant following the Fast-VESTAL procedure (Huang et al., 2014a) for a given frequency band.

The brain volume is pre-divided into a grid of dipoles with P nodes. Let $\mathbf{R}$ be the $M \times M$ sensor-waveform MEG covariance matrix where M is the number of MEG sensors for a given frequency band (e.g., beta band) and time-window (e.g., length of an epoch); and $\mathbf{G}$ be the $M \times 2P$ gain (lead-field) matrix calculated from MEG forward modeling for the pre-defined source grid with P dipole locations, with each dipole location having two orthogonal orientations (i.e., θ and ϕ). In the spherical MEG forward head model, θ and ϕ represent the two tangential orientations for each dipole location, whereas in a realistic MEG forward model using the Boundary Element Method (BEM), the θ and ϕ-orientations

are obtained as the two dominant orientations from the singular-value decomposition (SVD) of the $M \times 3$ lead-field matrix for each dipole, as previously documented (Huang et al., 2006).

Eigen-value decomposition is performed for the sensor-waveform covariance matrix:

$$R = U_B \Sigma_B U_B{}^T = U_B S_B S_B{}^T U_B{}^T \quad (1)$$

where the diagonal elements in $\mathbf{S}_B$ are simply the square root (SQRT) of the corresponding eigenvalues of $\mathbf{R}$ which are the diagonal elements in $\mathbf{\Sigma}_B$. Next, SVD is performed for the gain matrix $\mathbf{G}$:

$$G = U_G S_G V_G^T \quad (2)$$

The dimensions for $\mathbf{U}_G$, $\mathbf{S}_G$, and $\mathbf{V}_G$ are $M \times M$, $M \times 2P$, and $2P \times 2P$, respectively. Following the procedure in (Huang et al., 2014a), a distributed source solution for Eq. 2 can be expressed as:

$$U_B S_B = U_G S_G V_G^T H \quad (3)$$

The $2P \times M$ matrix $\mathbf{H}$ is called the distributed *source spatial map* matrix. The goal of MEG inverse source imaging is to obtain $\mathbf{H}$ for given $\mathbf{R}$ in Eq. 3. However, Eq. 3 is under-determined, with the number of unknown variables in each column of $\mathbf{H} = [\mathbf{h}_1,\mathbf{h}_2,\ldots,\mathbf{h}_k,\ldots,\mathbf{h}_M]$ (i.e., $2P$) much larger than the number of measurements in each column of $\mathbf{U}_B\mathbf{S}_B = [s_1\mathbf{u}_1,s_2\mathbf{u}_2,\ldots,s_k\mathbf{u}_k,\ldots,s_M\mathbf{u}_M,]$ (i.e., M), so additional constraint(s) are needed to obtain a unique solution for Eq. 3. Here, the number of signal (dominant) spatial modes k is usually much smaller than the number of MEG sensor measurements M. After multiplying from the left side with $\underline{\mathbf{U}}G^T$, for individual dominant spatial modes of Eq. 3, Eq. 3 can be written as:

$$U_G^T u_i s_i = S_G V_G^T h_i, i = 1, 2, \ldots, k \quad (4)$$

where $i = 1,2,\ldots,k$ are the indices of spatial modes in sensor space.

By introducing additional minimum L1-norm constraints (Huang et al., 2014a) to Eq. 4, one can obtain the Fast-VESTAL solution for $\mathbf{h}_i$:

$$\min(w^T|h_i|), \text{ subject to constraints } S_G V_G{}^T h_i \cong U_G^T u_i s_i, i = 1, 2, \ldots, k \quad (5)$$

where the $2P \times 1$ vector $\mathbf{h}_i$ is the source imaging map associated with the dominant spatial mode vector $\mathbf{u}_i$ (dimension $M \times 1$) of the sensor-domain. In Eq. 5, $w = \sqrt{diag(V_G V_G^T)}$ is a $2P \times 1$ weighting vector chosen to remove potential bias towards grid nodes at the superficial layer (Huang et al., 2014a). After solving for $\mathbf{h}_i$ and hence $\mathbf{H}$ using Eq. 5, the Fast-VESTAL source imaging result can be obtained on the source grid as:

$$A = \sqrt{diag(HH^T)} \quad (6)$$

which is the $2P \times 1$ source magnitude value across grid nodes. The main feature of $\mathbf{A}$, the Fast-VESTAL-based distributed source solution, is that it is highly sparse, with many of its elements being either zero or close to zero, as a direct consequence of L1-norm minimization. An Objective Pre-whitening Method was applied to remove correlated environmental noise and objectively select the dominant eigen-modes (i.e., k) of sensor-waveform covariance matrix (Huang et al., 2014a).

2.5. Statistical analysis of MEG source magnitude images

Statistical analysis was performed separately for each frequency band. MEG source magnitude imaging volumes obtained from Fast-VESTAL that cover the whole brain from all healthy control and PTSD participants were first spatially smoothed using a Gaussian kernel with 3 mm full width half maximum (FWHM), and then co-registered to an MNI-152 brain-atlas template using FLIRT program in FSL software package (http://www.fmrib.ox.ac.uk/fsl/). For each voxel in the MNI space, the MEG source magnitude data were run through a logarithm transformation. A two-tailed t-test was performed to assess the group difference for each voxel of the brain volume in the MNI space. False discovery rate (FDR) was used to control the family-wise error (Benjamini and Hochberg, 1995) with $q < .05$. The above procedure was performed for each of the frequency bands separately.

2.6. Correlation with symptom scores in PTSD

For brain areas that showed group differences within a specific frequency band, regions of interest (ROIs) were obtained by grouping the voxels together. We were specifically interested in the ROIs that covered amygdala, vmPFC, OFC, precuneous, and dlPFC. Within each ROI, we performed a correlational analysis between MEG source magnitude and PTSD symptom score. The analyses were performed in the 20 participants with PTSD or partial PTSD as measured by CAPS Total score. The remaining 5 participants with PTSD or partial PTSD as measured by PCL were not included in this correlational analysis.

3. Results

3.1. Beta-band MEG source magnitude imaging results

Fig. 1 shows group differences between participants with PTSD and healthy volunteers in resting-state MEG source magnitude for the beta-band (15–30 Hz). Increased beta-band activity in PTSD (hyperactivity, PTSD > controls) was generated from bilateral amygdala and left anterior hippocampus (white arrows), left and right posterolateral OFC (magenta arrows), several regions within the right insular cortex, bilateral middle temporal gyri, right posterior cingulate cortex (PCC, brown arrow), bilateral junctions of PCC and lingual gyri, and left occipito-temporal–parietal junction. In addition, Fig. 1 shows decreased beta-band activity in PTSD (hypoactivity, PTSD < controls) from vmPFC (green arrows) including rostral anterior cingulate cortex (rACC) and medial OFC, bilateral FPs (more R than L), bilateral caudate, bilateral dlPFC (more R than L), right superior frontal gyrus, mid-line supplementary motor areas (SMA), right anterior aspect of superior temporal gyrus, bilateral precuneous cortices, and bilateral sensorimotor cortices (more R than L). For a region, an asymmetry is reported when one hemisphere has twice or more voxels being significant than the equivalent region in the opposite hemisphere.

3.2. Gamma and high-gamma-bands MEG source magnitude imaging results

The upper panel of Fig. 2 shows increased gamma-band (30–80 Hz) activity in PTSD compared to the healthy control group that was generated from left and right posterolateral OFC (magenta arrows, more L than R), bilateral dmPFC including the dorsal paracingulate cortices and dorsal anterior cingulate cortex (dACC) (more L than R), several regions within the bilateral insular cortices, bilateral occipito-temporal–parietal junctions (more L than R), bilateral temporal–occipital fusiform cortices (more R than L), left occipital fusiform gyrus and right lingual gyrus, and right dorsomedial occipital cortex. The upper panel of Fig. 2 also shows decreased gamma-band activity in PTSD compared to the control group from vmPFC (green arrows) including rACC and medial OFC, bilateral FPs (more R than L), right dlPFC, mid-line SMA, and right sensorimotor cortices.

The lower panel of Fig. 2 shows increased high-gamma-band (80–150 Hz) activity in PTSD from left amygdala and hippocampus (white arrows), left posterolateral OFC (magenta arrows), right dACC, left FP, several regions within the bilateral insular cortices, bilateral occipito-temporal–parietal junctions (more L than R), and right dorsomedial occipital cortex. The lower panel of Fig. 2 also shows

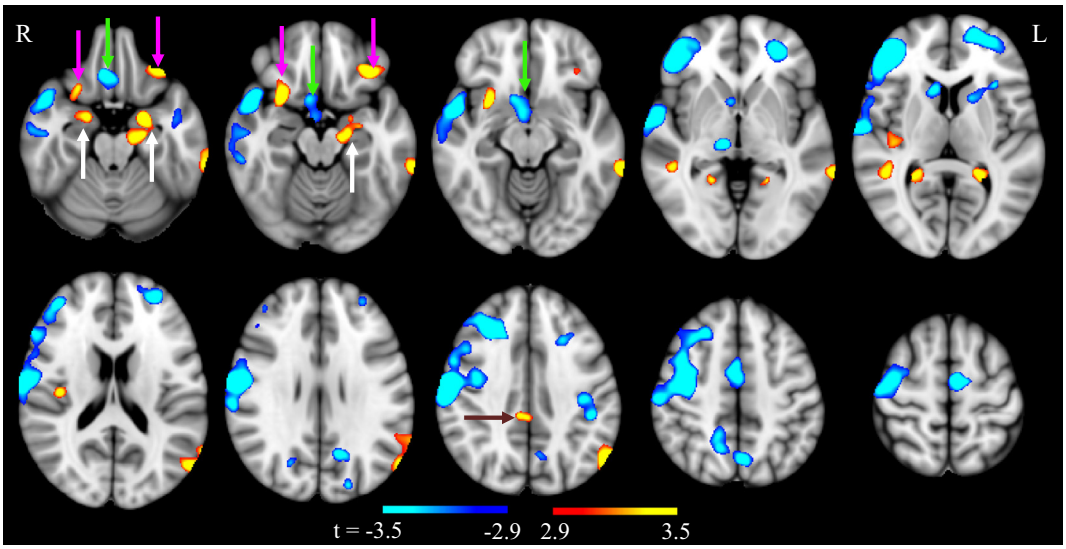

Fig. 1. Abnormal beta band (15–30 Hz) MEG activity in PTSD. Red-yellow color scale indicates increased (hyper-) activity in PTSD over health controls, whereas blue-cyan color scale indicates decreased (hypo-) activity in PTSD over health controls. White arrows: amygdala and hippocampus activity. Green arrows: vmPFC activity. Magenta arrows: posterolateral OFC activity. Brown arrow: PCC activity. The t-threshold of 2.9 is associated with FDR corrected $p < .05$.

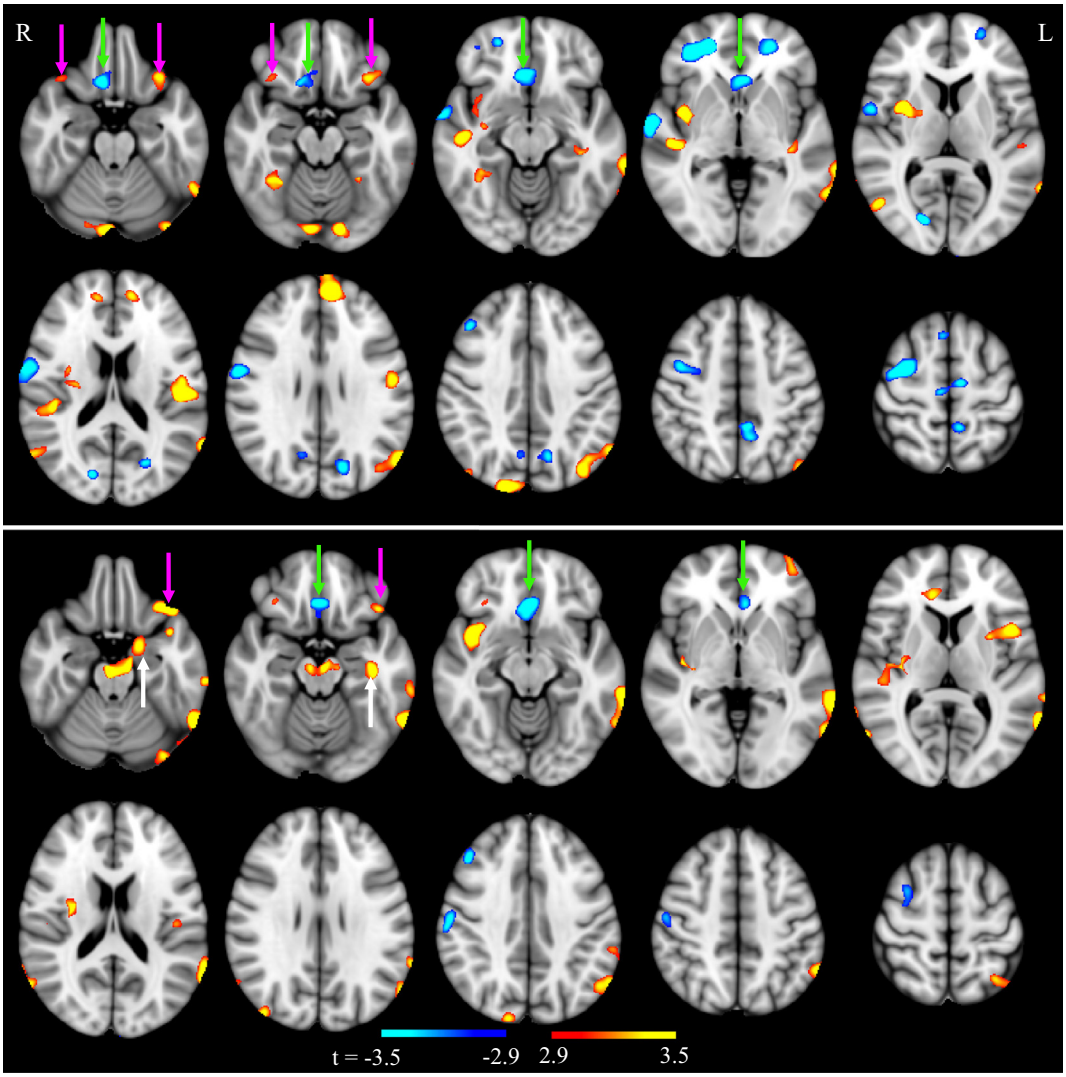

Fig. 2. Top panel: abnormal gamma band (30–80 Hz) MEG activity in PTSD; bottom panel: abnormal high-gamma band (80–150 Hz) MEG activity in PTSD. Red-yellow color scale indicates increased (hyper-) activity in PTSD over health controls, whereas blue-cyan color scale indicates decreased (hypo-) activity in PTSD over health controls. White arrows: amygdala and hippocampus activity. Green arrows: vmPFC activity. Magenta arrows: posterolateral OFC activity. The t-threshold of 2.9 is associated with FDR corrected $p < .05$.

decreased high-gamma-band activity in PTSD from mid-line vmPFC (green arrows) including rACC and medial OFC, right dlPFC, and right sensorimotor cortices.

3.3. Alpha and low-frequency bands MEG source magnitude imaging results

Although PTSD was associated with both hyper- and hypoactivity in the beta, gamma, and high-gamma bands, alpha band MEG activity was largely hypoactive in PTSD when compared with the healthy volunteers. The upper panel of Fig. 3 shows significantly decreased alpha-band activity in PTSD generated from bilateral FPs, bilateral dlPFC (more R than L), right superior frontal gyrus, bilateral anterior aspects of superior temporal gyri (more R than L), bilateral precuneous cortices, and bilateral sensorimotor cortices (more R than L). In contrast, only the left occipito-temporal–parietal junction showed increased alpha-band activity in PTSD.

PTSD was also strongly associated with hypoactivity in the low-frequency band compared to the healthy volunteers. The lower panel of Fig. 3 shows significantly decreased alpha-band activity in PTSD generated from bilateral FPs, bilateral dlPFC (more R than L), bilateral anterior aspects of superior temporal gyri (more R than L), bilateral precuneous cortices, and bilateral sensorimotor cortices (more R than L). Similar to the patterns observed in the alpha band, only the left occipito-temporal–parietal junction showed increased low-frequency-band activity in PTSD.

3.4. Results of MEG source magnitude correlating with PTSD symptoms

Positive correlations between resting-state MEG activity and CAPS Total symptom scores were found in left amygdala (beta band, $r = +0.51$, $p < .05$) and left posterolateral OFC (also in beta band, $r = +0.55$, $p < .05$), indicating the stronger the resting-state MEG activity in these areas, the more severe the PTSD symptoms. In addition, negative correlations between resting-state MEG activity and total CAPS symptom scores were found in midline vmPFC (beta band, $r = -0.58$, $p < .01$; gamma band, $r = -0.63$, $p < .01$; and high-gamma band, $r = -0.60$, $p < .01$), and midline precuneous (alpha band, $r = -0.48$, $p < .05$), indicating the weaker the resting-state MEG activity in these areas, the more severe the PTSD symptoms.

4. Discussion

For the first time to our knowledge, the present study shows that individuals with PTSD have abnormal electromagnetic activity that can be directly *imaged* by resting-state MEG source imaging technique for all

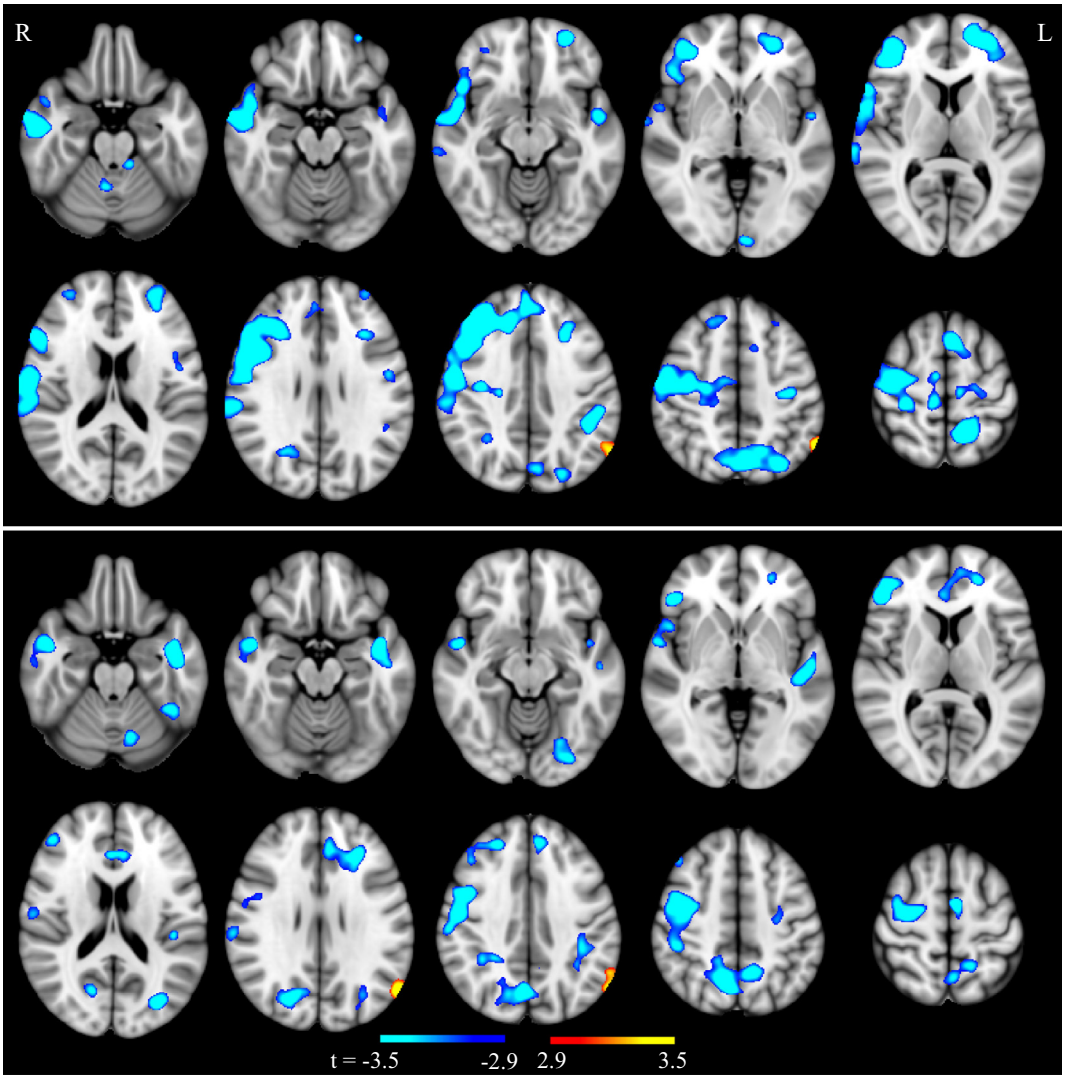

Fig. 3. Top panel: abnormal alpha band (8–12 Hz) MEG activity in PTSD; bottom panel: abnormal low-frequency band (1–7 Hz) MEG activity in PTSD. The t-threshold of 2.9 is associated with FDR corrected $p < .05$.

frequency bands. PTSD was associated with: 1) MEG hyperactivity from amygdala, hippocampus, posterolateral OFC, dmPFC, insular cortex, and PCC in high frequency bands (i.e., beta, gamma, and high gamma bands); 2) MEG hypoactivity from vmPFC, FP, and dlPFC in the high frequency bands; 3) extensive MEG hypoactivity from dlPFC, FP, anterior temporal lobes, precuneous cortex, and sensorimotor cortex in alpha and low-frequency bands, with dlPFC and sensorimotor cortex hypoactivity more prominent in right versus left hemispheres; and 4) resting-state MEG activity in left amygdala and posterolateral OFC positively correlated with PTSD symptom scores, whereas MEG activity in vmPFC and precuneous correlated negatively with the PTSD symptoms.

Neuronal activity from different frequency bands is considered to reflect different neuronal mechanisms. Thalamo-cortical interactions are essential for alpha rhythms, and normal alpha-band activity is associated with functional inhibition; specifically, increased alpha-band power in a brain area was linked to reduced functional connectivity with other brain areas (De Munck et al., 2009; Hindriks and van Putten, 2013; Scheeringa et al., 2012). Activity in the beta band is associated with communication between remote brain structures, whereas gamma synchrony promotes local computations (Kopell et al., 2000; Singer, 1999). Although the gamma band electromagnetic signals are generated locally, non-local brain areas can still show significant functional connectivity as measured by coherence related to the gamma band signals. Using combined electrophysiological and fMRI measurements, studies in both human and animals showed that gamma-band power exhibits spatial coherence over long timescales with the strongest coherence between functionally related areas that are not necessarily local (He et al., 2008; Nir et al., 2008; Scholvinck et al., 2010, 2013; Shmuel and Leopold, 2008). Unlike alpha-band activity, beta and gamma-band activity does not necessarily have to involve thalamus. Theta-band signals have been reported in previous EEG studies, although these signals were predominantly task-activated (e.g., problem solving) (Mizuki et al., 1980, 1984, 1992; Niedermeyer and Lopes da Silva, 2005; Takahashi et al., 1997). Increased low-frequency brain rhythms in delta band were often seen in individuals with neurological disorders, e.g. epilepsy and traumatic brain injury (Baayen et al., 2003; de Jongh et al., 2003; Decker and Knott, 1972; Huang et al., 2009, 2012, 2014b; Lewine et al., 1999; Lewine and Orrison, 1995; Nagata et al., 1985; Vieth et al., 1996). When examining the mechanism of abnormal delta rhythms, electrophysiological studies in animals show that abnormal delta activity is from gray matter neurons that have experienced deafferentation due to neurological injuries in underlying white matter, resulting from axonal injury or blockage/limitation in the cholinergic pathways (Ball et al., 1977; Gloor et al., 1977; Schaul et al., 1978; Schaul, 1998).

4.1. MEG findings in amygdala and hippocampus

Individuals with PTSD showed amygdala hyperactivity. Our MEG findings are consistent with previous PET and fMRI findings of hyperresponsive amygdala activity in PTSD (Rauch et al., 1998, 2006), which is one of the most robust functional neuroimaging findings in PTSD (Hughes and Shin, 2011). The amygdala is involved in processing threat-related stimuli (Davis and Whalen, 2001; Morris et al., 1998; Whalen et al., 1998, 2001) and is necessary for fear conditioning (Davis and Whalen, 2001; LeDoux, 2000; Shin et al., 2006). Moreover, the amygdala is a key component in the neurocircuitry model of PTSD (Rauch et al., 2006). The present MEG study shows that the amygdala hyperactivity in PTSD can also be detected using electromagnetic source imaging measures, which increases the confidence in our MEG technique for detecting new abnormalities in PTSD. Furthermore, we demonstrate that amygdala hyperactivity was only observable in the high frequency bands (i.e., beta and high-gamma bands). In addition, the MEG hyperactivity in PTSD from left hippocampus in beta and high-gamma bands is also consistent with the current PTSD neurocircuitry model (Rauch et al., 2006), although the findings from previous PET and fMRI in this region have been mixed (Hughes and Shin, 2011).

4.2. MEG findings in dmPFC and insula

The MEG gamma-band hyperactivity from dmPFC, including the dACC, in PTSD was also consistent with prior PET and fMRI findings (Bremner et al., 1999; Felmingham et al., 2009; Pannu et al., 2009; Shin et al., 2001, 2007, 2011). The dmPFC, including the dACC, is thought to play an important role in a variety of cognitive processes such as performance monitoring, response selection, error detection, and decision making (Shin et al., 2011). In addition, PTSD was associated with increased MEG insular activity. Our findings are consistent with studies that used trauma-event-script-driven imagery with SPECT (Lindauer et al., 2008) and fMRI (Lanius et al., 2007), as well as with studies that used emotional and trauma-unrelated stimuli with PET and fMRI (Hughes and Shin, 2011). Painful stimuli have also been shown to increase insular activity in PTSD (Geuze et al., 2007; Strigo et al., 2010). The insular cortex processes information about the body's internal state and contributes to the autonomic component of the overall pain response. It has been suggested that the insular cortex integrates the sensory, affective, and cognitive components necessary for normal responses to pain (Kandel et al., 2000). Abnormal insular activity in PTSD may reflect a deficit in integrating these components, thereby contributing to an abnormal pain response (Nagai et al., 2007).

4.3. MEG findings in vmPFC

MEG hypoactivity from vmPFC in PTSD was consistent with findings from PET and fMRI studies (Hughes and Shin, 2011; Rauch et al., 1998, 2006). Hyporesponsive vmPFC is another key component in the current neurocircuitry model of PTSD (Rauch et al., 2006), which suggests that hyporesponsive vmPFC fails to suppress the amygdala (Rauch et al., 2006; Shin et al., 2006). The vmPFC is connected to and receives input from the ventral tegmental area, amygdala, temporal lobe, olfactory system, and dorsomedial thalamus. In turn, vmPFC sends signals to amygdala, temporal lobe, lateral hypothalamus, hippocampal formation, cingulate cortex, and certain other regions of the prefrontal cortex (Carlson, 2013). In the present study, hypoactivity in vmPFC associated with PTSD was evident in beta, gamma, and high-gamma bands, but not the lower frequency bands. These findings suggest that the beta- and gamma-band interactions between vmPFC and amygdala may not involve thalamus, as evidenced by the lack of group differences in vmPFC in thalamus-dependent alpha band activity (Hindriks and van Putten, 2013).

4.4. Resting-state MEG versus resting-state fMRI

We used a resting-state protocol that is insensitive to stimulus features and participant performance. Furthermore, we focused on examining MEG source-magnitude images rather than functional connectivity (Jin et al., 2013). Our protocol was similar to a recent resting-state fMRI study of combat-related PTSD that used a magnitude imaging approach (Yan et al., 2013). Our findings are consistent with Yan and colleagues, who also found that individuals with PTSD showed increased activity in amygdala, insular cortex, and OFC, as well as decreased activity in dlPFC, superior frontal gyrus, and precuneous cortex. Despite these similarities, participants with PTSD in the present study showed *decreased* MEG activity in vmPFC (beta, gamma, and high-gamma bands, see Figs. 1 and 2) and bilateral FP areas (Figs. 1–3), whereas Yan and colleagues, in their fMRI study showed *increased* activity in a similar region (Yan et al., 2013). Although it is known that the fMRI measurements in ventral frontal lobe areas are challenging to obtain due to signal loss, imaging distortion, and susceptibility artifacts (Czervionke et al., 1988; Domsch et al., 2013), the exact reason of the decreased MEG versus increased fMRI resting-state activity in vmPFC is unknown.

Overall, the beta-band MEG source imaging maps are similar to the fMRI maps of Yan and colleagues, except for the activity in vmPFC. Such a degree of similarity across two different imaging modalities (i.e., electromagnetic measures from MEG and hemodynamic measures from fMRI) is likely due to beta-band synchronization over long conduction delays, which corresponds to signals traveling a significant distance across brain regions. Electrophysiological studies of the rat hippocampus have shown that the beta rhythm allows neuronal synchrony at large time delays, while the gamma band allows such synchrony at short delays. Thus, beta synchrony promotes communication between remote structures, whereas gamma synchrony promotes local computations (Kopell et al., 2000; Singer, 1999). Interestingly, more recent work in identifying MEG correlates of fMRI resting-state networks has found that power fluctuations in the beta band produce spatial networks very similar to fMRI resting-state networks (Brookes et al., 2011b). Our findings suggest that abnormal beta-band neuronal activity in PTSD is likely a candidate for the abnormal fMRI signal observed by Yan and colleagues (Yan et al., 2013).

The consistent finding of decreases of resting-state activity in precuneous and dlPFC associated with PTSD in the present MEG study (in beta, alpha, and low-frequency bands) and in the fMRI study by Yan et al. (Yan et al., 2013) highlight the contribution of these regions in PTSD neurocircuitry. The precuneous is a key region of the "default-mode network (DMN)" in resting brain which has been detected by fMRI (Fransson and Marrelec, 2008) and MEG (Brookes et al., 2011b). Furthermore, the precuneous plays a pivotal role in how intrinsic activity is mediated throughout the DMN, and helps sustain a sense of self-consciousness in self-referential mental thoughts during rest (Cavanna and Trimble, 2006; Fransson and Marrelec, 2008). Non-trauma related words elicit decreased precuneous fMRI activity in PTSD, and the decrease in precuneous activity is correlated with CAPS scores (Geuze et al., 2008). Dissociative symptoms of patients with PTSD may play a role in the decreased activation of precuneous (Geuze et al., 2008). The dlPFC is a key region for a variety of executive brain functions such as working memory, attention, and other executive functions. It facilitates goal-directed behavior through indirect modulation of the amygdala response to threat, possibly through connections with the temporal cortex (Bishop, 2008; Gold et al., 2014; Mitchell, 2011). In the present study, MEG hyperactivity in both right dlPFC and anterior temporal lobe in alpha, beta, gamma, and low-frequency (Figs. 1–3) is consistent with the modulation deficit of the dlPFC–anterior temporal-amygdala pathway in PTSD. Using a task involving cognitive regulation of negative affect via reappraisal, Rabinak and colleagues found that PTSD patients engaged the dlPFC during cognitive reappraisal, albeit to a lesser extent than the control participants (Rabinak et al., 2014). In a longitudinal cortical thickness study, individuals with PTSD showed greater dlPFC thickness in a follow-up exam about 1 year after the trauma than in the acute exam, and greater dlPFC thickness was associated with greater PTSD symptom reductions and better recovery (Lyoo et al., 2011). On the other hand, healthy volunteers showed greater dlPFC activation and increased amygdala connectivity to threats compared to non-threat condition (Gold et al., 2014). Elevated activity in dlPFC was also observed in PTSD during a maintenance period of working memory in an fMRI test (Moores et al., 2008). Future functional imaging studies of PTSD are needed to examine the association between resting-state dlPFC activity and dlPFC responses to different types of working memory and/or attention stimuli.

In an event related potential (ERP) study of combat veterans with PTSD after mild TBI by Shu and colleagues, PCC and precuneous areas exhibit greater ERPs evoked by emotional facial stimuli (Shu et al., 2014). In the present study, PCC also showed hyperactivity in the beta-band resting-state MEG source image (brown arrow in Fig. 1), a finding consistent with the above ERP study. However, the hypoactive precuneous is seen in our resting-state MEG source image across many frequency bands, also observed in resting-state fMRI by Yan and colleagues (Yan et al., 2013), seems to be different from the greater ERPs in precuneous found by Shu and colleagues using emotional stimuli. Additional studies are needed to directly examine the association between resting-state electromagnetic signal and evoked responses, as well as the impact of mild TBI on PTSD.

4.5. MEG findings in OFC

Another interesting finding from the present study is the increased activity from the posterolateral OFC areas in beta, gamma, and high gamma bands. Our finding is consistent with fMRI findings of increased resting-state activity in PTSD (Yan et al., 2013). The OFC is closely connected to the limbic system, especially the amygdala, and is sometimes regarded as part of the expanded limbic system (Nauta, 1979). While regions known to be part of the existing neurocircuitry model of PTSD (i.e., amygdala, vmPFC, and insular cortex) have been studied extensively (Rauch et al., 1998, 2006; Shin et al., 2006), the role of the posterolateral OFC in PTSD is unclear and should be examined further. Based on our MEG findings, posterolateral OFC activity increased with PTSD symptom severity, thus OFC and its interactions with the amygdala may be added to the existing neurocircuitry model of PTSD. This idea is supported by studies that show that OFC has direct anatomical projections to the amygdala and hippocampus via the uncinate fasciculus in humans (Bach et al., 2011; Talairach and Tournoux, 1988) as well as in non-human primates (Carmichael and Price, 1995). It was also shown that such projections were abnormal in some psychiatric disorders such as conduct disorder (Passamonti et al., 2012), bipolar disorder (Benedetti et al., 2011), and schizophrenia (Jackowski et al., 2012). Further studies are needed to confirm whether disrupted interactions between OFC-amygdala may be implicated in PTSD.

4.6. Decreased MEG alpha-band activity in PTSD

Individuals with PTSD showed extensive MEG alpha-band hypoactivity from dlPFC, FP, anterior temporal lobes, precuneous cortex, and sensorimotor cortex. Neuronal modeling studies showed that thalamo-cortical interactions are essential to the generation of alpha rhythms (Freyer et al., 2011; Hindriks and van Putten, 2013; Lopes da Silva et al., 1997). Combined EEG and fMRI studies have also shown that increased alpha-band power in a brain area is associated with reduced functional connectivity with other brain areas, suggesting that alpha-band activity is associated with functional inhibition (De Munck et al., 2009; Scheeringa et al., 2012). The observed MEG alpha-band hypoactivity may suggest a deficit in thalamo-cortical interactions, which possibly leads to reduced functional inhibition in the above cortical areas in PTSD. In general, a normal amount of alpha activity is preferred in the resting-state, and reduced alpha-band power has also been observed in individuals with Alzheimer's disease (Babiloni et al., 2013; Tartaglione et al., 2012), and schizophrenia (Hinkley et al., 2011; Sponheim et al., 2000).

4.7. MEG source imaging with fast-VESTAL

Our method plays an essential role in obtaining the source magnitude images for the neurocircuitry in PTSD (Figs. 1–3). It was shown that Fast-VESTAL can effectively create resting-state MEG source images that are highly consistent with known neurophysiology findings (Huang et al., 2014a). We have shown that for resting-state MEG signal, the source magnitude images obtained using a beamformer technique (a popular MEG source analysis method) are less consistent with neurophysiology findings (Huang et al., 2014a). This is likely due to beamformer's intrinsic limitation which assumes the neuronal sources are uncorrelated (Robinson and Vrba, 1999; Sekihara et al., 2001; Van Veen et al., 1997), a questionable assumption when dealing with resting-state MEG signals.

In the present study, we focus on MEG source magnitude images in PTSD. No results were presented regarding the MEG-based connectivity

analyses. This is because we are in the process of finalizing the Fast-VESTAL based voxel-wise MEG connectivity method (Huang et al., in preparation). Although MEG-based connectivity study is a hot topic in literature, with most published approaches used Beamformer or minimum L2-norm based techniques to obtain the source time-courses (Brookes et al., 2011a,b, 2012; Ghuman et al., 2011; Gramfort et al., 2014). It was known that source time-courses obtain by Beamformer are distorted when multiple correlated neuronal sources contribute to the sensor-waveforms even at noiseless cases (Huang et al., 2014a), and across-talk between source time-courses from minimum L2-norm approaches can also be a serious issue. However, even though many researchers were aware of the issues associated with distorted source time-courses, the impact on a variety of connectivity measures using the distorted source time-courses has not been examined thoroughly in resting-state data, at least to our knowledge. Before we publish our method for Fast-VESTAL based connectivity analysis, we believe that it would be beyond the scope of the present study to include MEG connectivity results for the PTSD population.

There are several limitations of the present study that warrant consideration. First, the spatial resolution and localization accuracy of MEG are expected to be limited for amygdala, hippocampus, and vmPFC, which may explain some minor location discrepancies between our findings and those of previous fMRI or PET studies. Second, although we acquired resting-state MEG signal in the eyes-closed condition, eye-movements and micro-eye-blinks may be confounding factors. Although we pre-processed the MEG data through both MaxFilter and ICA to remove the eye-movement and micro-eye-blinks, the impact of residual eye-activity-related artifacts may not be totally negligible. Third, despite substantial efforts to ensure and monitor alertness during the eyes-closed condition (see Materials and methods), drowsiness may still have had an impact on the MEG recording. Fourth, since the active-duty and veteran PTSD patients are mostly males, the present study is dominated by male subjects, with just one woman in each of the two groups.

Despite these limitations, the present study showed that our MEG source imaging technique revealed new abnormalities in the resting-state electromagnetic signals from PTSD neurocircuitry. Abnormal resting-state electromagnetic signals in PTSD neurocircuitry can be effectively imaged by MEG source imaging technique for different frequency bands. In high frequency bands (i.e., beta, gamma, and high gamma bands), PTSD was associated with 1) MEG hyperactivity from amygdala, hippocampus, posterolateral OFC, dmPFC, and insular cortex; and 2) MEG hypoactivity from vmPFC, FP, and dlPFC. In alpha and low-frequency bands, PTSD was associated with extensive MEG hypoactivity from dlPFC, FP, anterior temporal lobes, precuneous cortex, and sensorimotor cortex. Lastly, PTSD symptom scores correlated positively with resting-state MEG activity in left amygdala and posterolateral OFC and negatively with MEG activity in vmPFC and precuneous. Particularly, posterolateral OFC and precuneous may play important roles in the PTSD neurocircuitry model.

Acknowledgments

This work was supported in part by Headquarters Marine Corps and Navy BUMED to D.G. Baker, M.A. Geyer, M.X. Huang and V.B. Risbrough (MRS-II; Navy BUMED contract # N62645-11-C-4037) and Merit Review Grants from the Department of Veterans Affairs to M.X. Huang (I01-CX000499, NURC-022-10F, NEUC-044-06S). We acknowledge the MRS-II administrative core, Anjana Patel, Andrew De La Rosa, and members of the MRS-II Team, including logistic coordinators, clinician-interviewers, and data collection staff. We thank staff at the Veterans Medical Research Foundation (VRMF). We also thank the Marine, Navy and veteran volunteers for their military service and participation in this study.

References

American Psychiatric Association, 2000. Diagnostic and Statistical Manual of Mental Disorders IV, Text RevisionAmerican Psychiatric Association.
American Psychiatric Association, 2004. Practice Guideline for the Treatment of Patients With Acute Stress Disorder and PTSDAmerican Psychiatric Association, Arlington, VA.
Anderson, A.K., Christoff, K., Panitz, D., De Rosa, E., Gabrieli, J.D., 2003. Neural correlates of the automatic processing of threat facial signals. Journal of Neuroscience: the Official Journal of the Society for Neuroscience 23, 5627–5633 12843265.
Baayen, J.C., de Jongh, A., Stam, C.J., De Munck, J.C., Jonkman, J.J., Trenité, D.G., Berendse, H. W., van Walsum, A.M., Heimans, J.J., Puligheddu, M., Castelijns, J.A., Vandertop, W.P., 2003. Localization of slow wave activity in patients with tumor-associated epilepsy. Brain Topography 16, 85–93 14977201.
Babiloni, C., Del Percio, C., Bordet, R., Bourriez, J.L., Bentivoglio, M., Payoux, P., Derambure, P., Dix, S., Infarinato, F., Lizio, R., Triggiani, A.I., Richardson, J.C., Rossini, P.M., 2013. Effects of acetylcholinesterase inhibitors and memantine on resting-state electroencephalographic rhythms in Alzheimer's disease patients. Clinical Neurophysiology: Official Journal of the International Federation of Clinical Neurophysiology 124, 837–850. http://dx.doi.org/10.1016/j.clinph.2012.09.01723098644.
Bach, D.R., Behrens, T.E., Garrido, L., Weiskopf, N., Dolan, R.J., 2011. Deep and superficial amygdala nuclei projections revealed in vivo by probabilistic tractography. Journal of Neuroscience: the Official Journal of the Society for Neuroscience 31, 618–623. http://dx.doi.org/10.1523/JNEUROSCI.2744-10.201121228170.
Ball, G.J., Gloor, P., Schaul, N., 1977. The cortical electromicrophysiology of pathological delta waves in the electroencephalogram of cats. Electroencephalography and Clinical Neurophysiology 43, 346–361 70336.
Benedetti, F., Absinta, M., Rocca, M.A., Radaelli, D., Poletti, S., Bernasconi, A., Dallaspezia, S., Pagani, E., Falini, A., Copetti, M., Colombo, C., Comi, G., Smeraldi, E., Filippi, M., 2011. Tract-specific white matter structural disruption in patients with bipolar disorder. Bipolar Disorders 13, 414–424. http://dx.doi.org/10.1111/j.1399-5618.2011.00938.x21843281.
Benjamini, Y., Hochberg, Y., 1995. Controlling the false positive rate: a practical and powerful approach to multiple testing. Journal of the Royal Statistical Society, Series B 57, 289–300.
Bishop, S.J., 2008. Neural mechanisms underlying selective attention to threat. Annals of the New York Academy of Sciences 1129, 141–152. http://dx.doi.org/10.1196/annals.1417.01618591476.
Blake, D.D., Weathers, F.W., Nagy, L.M., Kaloupek, D.G., Gusman, F.D., Charney, D.S., Keane, T. M., 1995. The development of a Clinician-Administered PTSD Scale. Journal of Traumatic Stress 8, 75–90 7712061.
Blanchard, E.B., Hickling, E.J., Taylor, A.E., Forneris, C.A., Loos, W., Jaccard, J., 1995. Effects of varying scoring rules of the Clinician-Administered PTSD Scale (CAPS) for the diagnosis of post-traumatic stress disorder in motor vehicle accident victims. Behaviour Research and Therapy 33, 471–475 7755537.
Bremner, J.D., Narayan, M., Staib, L.H., Southwick, S.M., McGlashan, T., Charney, D.S., 1999. Neural correlates of memories of childhood sexual abuse in women with and without posttraumatic stress disorder. American Journal of Psychiatry 156, 1787–1795 10553744.
Brookes, M.J., Hale, J.R., Zumer, J.M., Stevenson, C.M., Francis, S.T., Barnes, G.R., Owen, J.P., Morris, P.G., Nagarajan, S.S., 2011a. Measuring functional connectivity using MEG: methodology and comparison with fcMRI. NeuroImage 56, 1082–1104. http://dx.doi.org/10.1016/j.neuroimage.2011.02.05421352925.
Brookes, M.J., Woolrich, M., Luckhoo, H., Price, D., Hale, J.R., Stephenson, M.C., Barnes, G.R., Smith, S.M., Morris, P.G., 2011b. Investigating the electrophysiological basis of resting state networks using magnetoencephalography. Proceedings of the National Academy of Sciences of the United States of America 108, 16783–16788. http://dx.doi.org/10.1073/pnas.111268510821930901.
Brookes, M.J., Woolrich, M.W., Barnes, G.R., 2012. Measuring functional connectivity in MEG: a multivariate approach insensitive to linear source leakage. NeuroImage 63, 910–920. http://dx.doi.org/10.1016/j.neuroimage.2012.03.04822484306.
Bryant, R.A., Felmingham, K.L., Kemp, A.H., Barton, M., Peduto, A.S., Rennie, C., Gordon, E., Williams, L.M., 2005. Neural networks of information processing in posttraumatic stress disorder: a functional magnetic resonance imaging study. Biological Psychiatry 58, 111–118. http://dx.doi.org/10.1016/j.biopsych.2005.03.02116038681.
Carlson, N.R., 2013. Physiology of BehavIOreleventh edition. Pearson, Boston.
Carmichael, S.T., Price, J.L., 1995. Limbic connections of the orbital and medial prefrontal cortex in macaque monkeys. Journal of Comparative Neurology 363, 615–641. http://dx.doi.org/10.1002/cne.9036304088847421.
Cavanna, A.E., Trimble, M.R., 2006. The precuneus: a review of its functional anatomy and behavioural correlates. Brain: A Journal of Neurology 129, 564–583. http://dx.doi.org/10.1093/brain/awl00416399806.
Chung, Y.A., Kim, S.H., Chung, S.K., Chae, J.H., Yang, D.W., Sohn, H.S., Jeong, J., 2006. Alterations in cerebral perfusion in posttraumatic stress disorder patients without re-exposure to accident-related stimuli. Clinical Neurophysiology: Official Journal of the International Federation of Clinical Neurophysiology 117, 637–642. http://dx.doi.org/10.1016/j.clinph.2005.10.02016426890.
Cohen, D., Schläpfer, U., Ahlfors, S., Hämäläinen, M., Halgren, E., 2002. New six-layer magnetically-shielded room for MEG. In: Nowak, H.H.J., Gießler, F. (Eds.), Proceedings of the 13th International Conference on Biomagnetism. Vde Verlag, Jena, Germany.
Corcoran, K.A., Maren, S., 2001. Hippocampal inactivation disrupts contextual retrieval of fear memory after extinction. Journal of Neuroscience: the Official Journal of the Society for Neuroscience 21, 1720–1726 11222661.
Czervionke, L.F., Daniels, D.L., Wehrli, F.W., Mark, L.P., Hendrix, L.E., Strandt, J.A., Williams, A. L., Haughton, V.M., 1988. Magnetic susceptibility artifacts in gradient-recalled echo MR imaging. American Journal of Neuroradiology 9, 1149–1155 3143237.
Davis, M., Whalen, P.J., 2001. The amygdala: vigilance and emotion. Molecular Psychiatry 6, 13–34 11244481.

de Jongh, A., Baayen, J.C., De Munck, J.C., Heethaar, R.M., Vandertop, W.P., Stam, C.J., 2003. The influence of brain tumor treatment on pathological delta activity in MEG. NeuroImage 20, 2291–2301 14683730.
De Munck, J.C., Gonçalves, S.I., Mammoliti, R., Heethaar, R.M., Lopes da Silva, F.H., 2009. Interactions between different EEG frequency bands and their effect on alpha-fMRI correlations. NeuroImage 47, 69–76. http://dx.doi.org/10.1016/j.neuroimage.2009.04.02919376236.
Decker Jr., D.A., Knott, J.R., 1972. The EEG in intrinsic supratentorial brain tumors: a comparative evaluation. Electroencephalography and Clinical Neurophysiology 33, 303–310 4114914.
Dikmen, S.S., Ross, B.L., Machamer, J.E., Temkin, N.R., 1995. One year psychosocial outcome in head injury. Journal of the International Neuropsychological Society: JINS 1, 67–77 9375211.
Dohrenwend, B.P., Turner, J.B., Turse, N.A., Adams, B.G., Koenen, K.C., Marshall, R., 2006. The psychological risks of Vietnam for U.S. veterans: a revisit with new data and methods. Science (New York, N.Y.) 313, 979–982. http://dx.doi.org/10.1126/science.112894416917066.
Dolcos, F., LaBar, K.S., Cabeza, R., 2004. Interaction between the amygdala and the medial temporal lobe memory system predicts better memory for emotional events. Neuron 42, 855–863 15182723.
Domsch, S., Linke, J., Heiler, P.M., Kroll, A., Flor, H., Wessa, M., Schad, L.R., 2013. Increased BOLD sensitivity in the orbitofrontal cortex using slice-dependent echo times at 3 T. Magnetic Resonance Imaging 31, 201–211. http://dx.doi.org/10.1016/j.mri.2012.06.02022925606.
Engdahl, B., Leuthold, A.C., Tan, H.-R.M., Lewis, S.M., Winskowski, A.M., Dikel, T.N., Georgopoulos, A.P., 2010. Post-traumatic stress disorder: a right temporal lobe syndrome? Journal of Neural Engineering 7, 066005. http://dx.doi.org/10.1088/1741-2560/7/6/06600520980718.
Felmingham, K.L., Williams, L.M., Kemp, A.H., Rennie, C., Gordon, E., Bryant, R.A., 2009. Anterior cingulate activity to salient stimuli is modulated by autonomic arousal in post-traumatic stress disorder. Psychiatry Research 173, 59–62. http://dx.doi.org/10.1016/j.pscychresns.2008.12.00519446442.
Fransson, P., Marrelec, G., 2008. The precuneus/posterior cingulate cortex plays a pivotal role in the default mode network: evidence from a partial correlation network analysis. NeuroImage 42, 1178–1184. http://dx.doi.org/10.1016/j.neuroimage.2008.05.05918598773.
Freyer, F., Roberts, J.A., Becker, R., Robinson, P.A., Ritter, P., Breakspear, M., 2011. Biophysical mechanisms of multistability in resting-state cortical rhythms. Journal of Neuroscience: the Official Journal of the Society for Neuroscience 31, 6353–6361. http://dx.doi.org/10.1523/JNEUROSCI.6693-10.201121525275.
Georgopoulos, A.P., Tan, H.-R.M., Lewis, S.M., Leuthold, A.C., Winskowski, A.M., Lynch, J.K., Engdahl, B., 2010. The synchronous neural interactions test as a functional neuromarker for post-traumatic stress disorder (PTSD): a robust classification method based on the bootstrap. Journal of Neural Engineering 7, 16011. http://dx.doi.org/10.1088/1741-2560/7/1/01601120086271.
Geuze, E., Vermetten, E., de Kloet, C.S., Westenberg, H.G., 2008. Precuneal activity during encoding in veterans with posttraumatic stress disorder. Progress in Brain Research 167, 293–297. http://dx.doi.org/10.1016/S0079-6123(07)67026-518037028.
Geuze, E., Westenberg, H.G., Jochims, A., de Kloet, C.S., Bohus, M., Vermetten, E., Schmahl, C., 2007. Altered pain processing in veterans with posttraumatic stress disorder. Archives of General Psychiatry 64, 76–85. http://dx.doi.org/10.1001/archpsyc.64.1.7617199057.
Ghuman, A.S., McDaniel, J.R., Martin, A., 2011. A wavelet-based method for measuring the oscillatory dynamics of resting-state functional connectivity in MEG. NeuroImage 56, 69–77. http://dx.doi.org/10.1016/j.neuroimage.2011.01.04621256967.
Gloor, P., Ball, G., Schaul, N., 1977. Brain lesions that produce delta waves in the EEG. Neurology 27, 326–333557774.
Gold, A.L., Morey, R.A., McCarthy, G., 2014. Amygdala-prefrontal cortex functional connectivity during threat-induced anxiety and goal-distractionBiological Psychiatry (in press).
Gramfort, A., Luessi, M., Larson, E., Engemann, D.A., Strohmeier, D., Brodbeck, C., Parkkonen, L., Hämäläinen, M.S., 2014. MNE software for processing MEG and EEG data. NeuroImage 86, 446–460. http://dx.doi.org/10.1016/j.neuroimage.2013.10.02724161808.
Hartley, C.A., Phelps, E.A., 2010. Changing fear: the neurocircuitry of emotion regulation. Neuropsychopharmacology: Official Publication of the American College of Neuropsychopharmacology 35, 136–146. http://dx.doi.org/10.1038/npp.2009.12119710632.
He, B.J., Snyder, A.Z., Zempel, J.M., Smyth, M.D., Raichle, M.E., 2008. Electrophysiological correlates of the brain's intrinsic large-scale functional architecture. Proceedings of the National Academy of Sciences of the United States of America 105, 16039–16044. http://dx.doi.org/10.1073/pnas.080701010518843113.
Hindriks, R., van Putten, M.J., 2013. Thalamo-cortical mechanisms underlying changes in amplitude and frequency of human alpha oscillations. NeuroImage 70, 150–163. http://dx.doi.org/10.1016/j.neuroimage.2012.12.01823266701.
Hinkley, L.B., Vinogradov, S., Guggisberg, A.G., Fisher, M., Findlay, A.M., Nagarajan, S.S., 2011. Clinical symptoms and alpha band resting-state functional connectivity imaging in patients with schizophrenia: implications for novel approaches to treatment. Biological Psychiatry 70, 1134–1142. http://dx.doi.org/10.1016/j.biopsych.2011.06.02921861988.
Hoge, C.W., Castro, C.A., Messer, S.C., McGurk, D., Cotting, D.I., Koffman, R.L., 2004. Combat duty in Iraq and Afghanistan, mental health problems, and barriers to care. New England Journal of Medicine 351, 13–22. http://dx.doi.org/10.1056/NEJMoa040603152293O3.
Hoge, C.W., McGurk, D., Thomas, J.L., Cox, A.L., Engel, C.C., Castro, C.A., 2008. Mild traumatic brain injury in U.S. soldiers returning from Iraq. New England Journal of Medicine 358, 453–463. http://dx.doi.org/10.1056/NEJMoa07297218234750.
Huang, M.X., Dale, A.M., Song, T., Halgren, E., Harrington, D.L., Podgorny, I., Canive, J.M., Lewis, S., Lee, R.R., 2006. Vector-based spatial-temporal minimum L1-norm solution for MEG. NeuroImage 31, 1025–1037. http://dx.doi.org/10.1016/j.neuroimage.2006.01.02916542857.
Huang, M.X., Huang, C.W., Robb, A., Angeles, A., Nichols, S.L., Baker, D.G., Song, T., Harrington, D.L., Theilmann, R.J., Srinivasan, R., Heister, D., Diwakar, M., Canive, J.M., Edgar, J.C., Chen, Y.H., Ji, Z., Shen, M., El-Gabalawy, F., Levy, M., McLay, R., Webb-Murphy, J., Liu, T.T., Drake, A., Lee, R.R., 2014a. MEG source imaging method using fast L1 minimum-norm and its applications to signals with brain noise and human resting-state source amplitude images. NeuroImage 84, 585–604. http://dx.doi.org/10.1016/j.neuroimage.2013.09.02224055704.
Huang, M.X., Nichols, S., Baker, D.G., Robb, A., Angeles, A., Yurgil, K.A., Drake, A., Levy, M., Song, T., McLay, R., Theilmann, R.J., Diwakar, M., Risbrough, V.B., Ji, Z., Huang, C.W., Chang, D.G., Harrington, D.L., Muzzatti, L., Canive, J.M., Christopher Edgar, J., Chen, Y.H., Lee, R.R., 2014b. Single-subject-based whole-brain MEG slow-wave imaging approach for detecting abnormality in patients with mild traumatic brain injury. NeuroImage. Clinical 5, 109–119. http://dx.doi.org/10.1016/j.nicl.2014.06.00425009772.
Huang, M.X., Nichols, S., Robb, A., Angeles, A., Drake, A., Holland, M., Asmussen, S., D'Andrea, J., Chun, W., Levy, M., Cui, L., Song, T., Baker, D.G., Hammer, P., McLay, R., Theilmann, R.J., Coimbra, R., Diwakar, M., Boyd, C., Neff, J., Liu, T.T., Webb-Murphy, J., Farinpour, R., Cheung, C., Harrington, D.L., Heister, D., Lee, R.R., 2012. An automatic MEG low-frequency source imaging approach for detecting injuries in mild and moderate TBI patients with blast and non-blast causes. NeuroImage 61, 1067–1082. http://dx.doi.org/10.1016/j.neuroimage.2012.04.02922542638.
Huang, M.X., Song, T., Hagler Jr., D.J., Podgorny, I., Jousmaki, V., Cui, L., Gaa, K., Harrington, D.L., Dale, A.M., Lee, R.R., Elman, J., Halgren, E., 2007. A novel integrated MEG and EEG analysis method for dipolar sources. NeuroImage 37, 731–748. http://dx.doi.org/10.1016/j.neuroimage.2007.06.00217658272.
Huang, M.X., Theilmann, R.J., Robb, A., Angeles, A., Nichols, S., Drake, A., D'Andrea, J., Levy, M., Holland, M., Song, T., Ge, S., Hwang, E., Yoo, K., Cui, L., Baker, D.G., Trauner, D., Coimbra, R., Lee, R.R., 2009. Integrated imaging approach with MEG and DTI to detect mild traumatic brain injury in military and civilian patients. Journal of Neurotrauma 26, 1213–1226. http://dx.doi.org/10.1089/neu.2008.067219385722.
Hughes, K.C., Shin, L.M., 2011. Functional neuroimaging studies of post-traumatic stress disorder. Expert Review of Neurotherapeutics 11, 275–285. http://dx.doi.org/10.1586/ern.10.19821306214.
Iversen, A.C., Fear, N.T., Ehlers, A., Hacker Hughes, J., Hull, L., Earnshaw, M., Greenberg, N., Rona, R., Wessely, S., Hotopf, M., 2008. Risk factors for post-traumatic stress disorder among UK armed forces personnel. Psychological Medicine 38, 511–522. http://dx.doi.org/10.1017/S003329170800277818226287.
Jackowski, A.P., Araújo Filho, G.M., Almeida, A.G., Araújo, C.M., Reis, M., Nery, F., Batista, I.R., Silva, I., Lacerda, A.L., 2012. The involvement of the orbitofrontal cortex in psychiatric disorders: an update of neuroimaging findings. Revista Brasileira de Psiquiatria (São Paulo, Brazil: 1999) 34, 207–212 22729418.
Jin, C., Qi, R., Yin, Y., Hu, X., Duan, L., Xu, Q., Zhang, Z., Zhong, Y., Feng, B., Xiang, H., Gong, Q., Liu, Y., Lu, G., Li, L., 2013. Abnormalities in whole-brain functional connectivity observed in treatment-naive post-traumatic stress disorder patients following an earthquake. Psychological Medicine 1–10 http://dx.doi.org/10.1017/S003329171300250X24168716.
Kandel, E.R., Schwartz, J.H., Jessell, T.M., 2000. Principles of Neural ScienceFourth edition. McGraw-Hill, New York.
Kessler, R.C., Berglund, P., Demler, O., Jin, R., Merikangas, K.R., Walters, E.E., 2005. Lifetime prevalence and age-of-onset distributions of DSM-IV disorders in the National Comorbidity Survey Replication. Archives of General Psychiatry 62, 593–602. http://dx.doi.org/10.1001/archpsyc.62.6.59315939837.
Kessler, R.C., Sonnega, A., Bromet, E., Hughes, M., Nelson, C.B., 1995. Posttraumatic stress disorder in the National Comorbidity Survey. Archives of General Psychiatry 52, 1048–1060 7492257.
Kopell, N., Ermentrout, G.B., Whittington, M.A., Traub, R.D., 2000. Gamma rhythms and beta rhythms have different synchronization properties. Proceedings of the National Academy of Sciences of the United States of America 97, 1867–1872 10677548.
Lanius, R.A., Frewen, P.A., Girotti, M., Neufeld, R.W., Stevens, T.K., Densmore, M., 2007. Neural correlates of trauma script-imagery in posttraumatic stress disorder with and without comorbid major depression: a functional MRI investigation. Psychiatry Research 155, 45–56. http://dx.doi.org/10.1016/j.pscychresns.2006.11.00617412567.
Leahy, R.M., Mosher, J.C., Spencer, M.E., Huang, M.X., Lewine, J.D., 1998. A study of dipole localization accuracy for MEG and EEG using a human skull phantom. Electroencephalography and Clinical Neurophysiology 107, 159–173 9751287.
LeDoux, J.E., 2000. Emotion circuits in the brain. Annual Review of Neuroscience 23, 155–184. http://dx.doi.org/10.1146/annurev.neuro.23.1.15510845062.
Lewine, J.D., Davis, J.T., Sloan, J.H., Kodituwakku, P.W., Orrison Jr., W.W., 1999. Neuromagnetic assessment of pathophysiologic brain activity induced by minor head trauma. AJNR. American Journal of Neuroradiology 20, 857–866 10369357.
Lewine, J.D., Orrison Jr., W.W., 1995. Spike and slow wave localization by magnetoencephalography. Neuroimaging Clinics of North America 5, 575–596 8564285.
Lindauer, R.J., Booij, J., Habraken, J.B., van Meijel, E.P., Uylings, H.B., Olff, M., Carlier, I.V., den Heeten, G.J., van Eck-Smit, B.L., Gersons, B.P., 2008. Effects of psychotherapy on regional cerebral blood flow during trauma imagery in patients with post-traumatic stress disorder: a randomized clinical trial. Psychological Medicine 38, 543–554. http://dx.doi.org/10.1017/S003329170700143217803835.
Logothetis, N.K., 2003. The underpinnings of the BOLD functional magnetic resonance imaging signal. Journal of Neuroscience: the Official Journal of the Society for Neuroscience 23, 3963–3971 12764080.
Lopes da Silva, F.H., Pijn, J.P., Velis, D., Nijssen, P.C., 1997. Alpha rhythms: noise, dynamics and models. International Journal of Psychophysiology: Official Journal of the International Organization of Psychophysiology 26, 237–249 9203006.

Lyoo, I.K., Kim, J.E., Yoon, S.J., Hwang, J., Bae, S., Kim, D.J., 2011. The neurobiological role of the dorsolateral prefrontal cortex in recovery from trauma. Longitudinal brain imaging study among survivors of the south Korean subway disaster. Archives of General Psychiatry 68, 701–713. http://dx.doi.org/10.1001/archgenpsychiatry.2011.7021727254.

Magruder, K.M., Yeager, D.E., 2009. The prevalence of PTSD across War eras and the effect of deployment on PTSD: a systematic review and meta-analysis. Psychiatric Annals 39, 778–788.

McGaugh, J.L., 2004. The amygdala modulates the consolidation of memories of emotionally arousing experiences. Annual Review of Neuroscience 27, 1–28. http://dx.doi.org/10.1146/annurev.neuro.27.070203.144157.15217324.

Mitchell, D.G., 2011. The nexus between decision making and emotion regulation: a review of convergent neurocognitive substrates. Behavioural Brain Research 217, 215–231. http://dx.doi.org/10.1016/j.bbr.2010.10.03021055420.

Mizuki, Y., Kajimura, N., Kai, S., Suetsugi, M., Ushijima, I., Yamada, M., 1992. Differential responses to mental stress in high and low anxious normal humans assessed by frontal midline theta activity. International Journal of Psychophysiology: Official Journal of the International Organization of Psychophysiology 12, 169–178 1592670.

Mizuki, Y., Kajimura, N., Nishikori, S., Imaizumi, J., Yamada, M., 1984. Appearance of frontal midline theta rhythm and personality traits. Folia Psychiatrica et Neurologica Japonica 38, 451–458 6535746.

Mizuki, Y., Tanaka, M., Isozaki, H., Nishijima, H., Inanaga, K., 1980. Periodic appearance of theta rhythm in the frontal midline area during performance of a mental task. Electroencephalography and Clinical Neurophysiology 49, 345–351 6158411.

Moores, K.A., Clark, C.R., McFarlane, A.C., Brown, G.C., Puce, A., Taylor, D.J., 2008. Abnormal recruitment of working memory updating networks during maintenance of traumaneutral information in post-traumatic stress disorder. Psychiatry Research 163, 156–170. http://dx.doi.org/10.1016/j.pscychresns.2007.08.01118455372.

Morris, J.S., Ohman, A., Dolan, R.J., 1998. Conscious and unconscious emotional learning in the human amygdala. Nature 393, 467–470. http://dx.doi.org/10.1038/309769624001.

Mosher, J.C., Leahy, R.M., Lewis, P.S., 1999. EEG and MEG: forward solutions for inverse methods. IEEE Transactions on Bio-Medical Engineering 46, 245–259 10097460.

Nagai, M., Kishi, K., Kato, S., 2007. Insular cortex and neuropsychiatric disorders: a review of recent literature. European Psychiatry: the Journal of the Association of European Psychiatrists 22, 387–394. http://dx.doi.org/10.1016/j.eurpsy.2007.02.00617416488.

Nagata, K., Gross, C.E., Kindt, G.W., Geier, J.M., Adey, G.R., 1985. Topographic electroencephalographic study with power ratio index mapping in patients with malignant brain tumors. Neurosurgery 17, 613–619 4058699.

Nauta, W.J.H., 1979. Expanding borders of the limbic system concept. In: Rasmussen, I., Marino, R. (Eds.), Functional Neurosurgery. Raven, New York, pp. 7–23.

Niedermeyer, E., Lopes da Silva, F.H., 2005. Electroencephalography: Basic Principles, Clinical Applications, and Related FieldsFifth edition. Lippincott Williams & Wilkins, Philadelphia.

Nir, Y., Mukamel, R., Dinstein, I., Privman, E., Harel, M., Fisch, L., Gelbard-Sagiv, H., Kipervasser, S., Andelman, F., Neufeld, M.Y., Kramer, U., Arieli, A., Fried, I., Malach, R., 2008. Interhemispheric correlations of slow spontaneous neuronal fluctuations revealed in human sensory cortex. Nature Neuroscience 11, 1100–1108 19160509.

Oken, B.S., Salinsky, M.C., Elsas, S.M., 2006. Vigilance, alertness, or sustained attention: physiological basis and measurement. Clinical Neurophysiology: Official Journal of the International Federation of Clinical Neurophysiology 117, 1885–1901. http://dx.doi.org/10.1016/j.clinph.2006.01.01716581292.

Pannu Hayes, J., LaBar, K.S., Petty, C.M., McCarthy, G., Morey, R.A., 2009. Alterations in the neural circuitry for emotion and attention associated with posttraumatic stress symptomatology. Psychiatry Research 172, 7–15. http://dx.doi.org/10.1016/j.pscychresns.2008.05.00519237269.

Passamonti, L., Fairchild, G., Fornito, A., Goodyer, I.M., Nimmo-Smith, I., Hagan, C.C., Calder, A.J., 2012. Abnormal anatomical connectivity between the amygdala and orbitofrontal cortex in conduct disorder. PloS One 7, e48789. http://dx.doi.org/10.1371/journal.pone.004878923144970.

Rabinak, C.A., Macnamara, A., Kennedy, A.E., Angstadt, M., Stein, M.B., Liberzon, I., Phan, K.L., 2014. Focal and aberrant prefrontal engagement during emotion regulation in veterans with posttraumatic stress disorderDepression and Anxiety (in press) 24677490.

Rauch, S.L., Shin, L.M., Phelps, E.A., 2006. Neurocircuitry models of posttraumatic stress disorder and extinction: Human neuroimaging research — past, present, and future. Biological Psychiatry 60, 376–382. http://dx.doi.org/10.1016/j.biopsych.2006.06.00416919525.

Rauch, S.L., Shin, L.M., Whalen, P.J., Pitman, R.K., 1998. Neuroimaging and the neuroanatomy of PTSD. C.N.S. Spectrums 3 (Suppl. 2), 30–41.

Renshaw, K.D., 2011. An integrated model of risk and protective factors for postdeployment PTSD symptoms in OEF/OIF era combat veterans. Journal of Affective Disorders 128, 321–326. http://dx.doi.org/10.1016/j.jad.2010.07.02220692705.

Robinson, S.E., Vrba, J., 1999. Functional neuroimaging by synthetic aperture magnetometry (SAM). In: Yoshimoto, T., Kotani, M., Kuriki, S., Karibe, H., Nakasato, N. (Eds.), Recent Advances in Biomagnetism. Tohoku University Press, Sendai, Japan, pp. 302–305.

Rosen, G.M., Lilienfeld, S.O., 2008. Posttraumatic stress disorder: an empirical evaluation of core assumptions. Clinical Psychology Review 28, 837–868. http://dx.doi.org/10.1016/j.cpr.2007.12.00218329146.

Schaul, N., 1998. The fundamental neural mechanisms of electroencephalography. Electroencephalography and Clinical Neurophysiology 106, 101–107 9741769.

Schaul, N., Gloor, P., Ball, G., Gotman, J., 1978. The electromicrophysiology of delta waves induced by systemic atropine. Brain Research 143, 475–486 647373.

Scheeringa, R., Petersson, K.M., Kleinschmidt, A., Jensen, O., Bastiaansen, M.C., 2012. EEG alpha power modulation of fMRI resting-state connectivity. Brain Connectivity 2, 254–264. http://dx.doi.org/10.1089/brain.2012.008822938826.

Schölvinck, M.L., Leopold, D.A., Brookes, M.J., Khader, P.H., 2013. The contribution of electrophysiology to functional connectivity mapping. NeuroImage 80, 297–306. http://dx.doi.org/10.1016/j.neuroimage.2013.04.01023587686.

Schölvinck, M.L., Maier, A., Ye, F.Q., Duyn, J.H., Leopold, D.A., 2010. Neural basis of global resting-state fMRI activity. Proceedings of the National Academy of Sciences of the United States of America 107, 10238–10243. http://dx.doi.org/10.1073/pnas.091311010720439733.

Sekihara, K., Nagarajan, S.S., Poeppel, D., Marantz, A., Miyashita, Y., 2001. Reconstructing spatio-temporal activities of neural sources using an MEG vector beamformer technique. IEEE Transactions on Bio-Medical Engineering 48, 760–771. http://dx.doi.org/10.1109/10.93090111442288.

Semple, W.E., Goyer, P.F., McCormick, R., Donovan, B., Muzic Jr., R.F., Rugle, L., McCutcheon, K., Lewis, C., Liebling, D., Kowaliw, S., Vapenik, K., Semple, M.A., Flener, C.R., Schulz, S.C., 2000. Higher brain blood flow at amygdala and lower frontal cortex blood flow in PTSD patients with comorbid cocaine and alcohol abuse compared with normals. Psychiatry 63, 65–74 10855761.

Shin, L.M., Bush, G., Milad, M.R., Lasko, N.B., Brohawn, K.H., Hughes, K.C., Macklin, M.L., Gold, A.L., Karpf, R.D., Orr, S.P., Rauch, S.L., Pitman, R.K., 2011. Exaggerated activation of dorsal anterior cingulate cortex during cognitive interference: a monozygotic twin study of posttraumatic stress disorder. American Journal of Psychiatry 168, 979–985. http://dx.doi.org/10.1176/appi.ajp.2011.0912181221724666.

Shin, L.M., Bush, G., Whalen, P.J., Handwerger, K., Cannistraro, P.A., Wright, C.I., Martis, B., Macklin, M.L., Lasko, N.B., Orr, S.P., Pitman, R.K., Rauch, S.L., 2007. Dorsal anterior cingulate function in posttraumatic stress disorder. Journal of Traumatic Stress 20, 701–712. http://dx.doi.org/10.1002/jts.2023117955522.

Shin, L.M., Liberzon, I., 2010. The neurocircuitry of fear, stress, and anxiety disorders. Neuropsychopharmacology: Official Publication of the American College of Neuropsychopharmacology 35, 169–191. http://dx.doi.org/10.1038/npp.2009.8319625997.

Shin, L.M., Orr, S.P., Carson, M.A., Rauch, S.L., Macklin, M.L., Lasko, N.B., Peters, P.M., Metzger, L.J., Dougherty, D.D., Cannistraro, P.A., Alpert, N.M., Fischman, A.J., Pitman, R.K., 2004a. Regional cerebral blood flow in the amygdala and medial prefrontal cortex during traumatic imagery in male and female Vietnam veterans with PTSD. Archives of General Psychiatry 61, 168–176. http://dx.doi.org/10.1001/archpsyc.61.2.16814757593.

Shin, L.M., Rauch, S.L., Pitman, R.K., 2006. Amygdala, medial prefrontal cortex, and hippocampal function in PTSD. Annals of the New York Academy of Sciences 1071, 67–79. http://dx.doi.org/10.1196/annals.1364.00716891563.

Shin, L.M., Shin, P.S., Heckers, S., Krangel, T.S., Macklin, M.L., Orr, S.P., Lasko, N., Segal, E., Makris, N., Richert, K., Levering, J., Schacter, D.L., Alpert, N.M., Fischman, A.J., Pitman, R.K., Rauch, S.L., 2004b. Hippocampal function in posttraumatic stress disorder. Hippocampus 14, 292–300.

Shin, L.M., Whalen, P.J., Pitman, R.K., Bush, G., Macklin, M.L., Lasko, N.B., Orr, S.P., McInerney, S.C., Rauch, S.L., 2001. An fMRI study of anterior cingulate function in posttraumatic stress disorder. Biological Psychiatry 50, 932–942 11750889.

Shmuel, A., Leopold, D.A., 2008. Neuronal correlates of spontaneous fluctuations in fMRI signals in monkey visual cortex: implications for functional connectivity at rest. Human Brain Mapping 29, 751–761. http://dx.doi.org/10.1002/hbm.2058018465799.

Shu, I.W., Onton, J.A., Prabhakar, N., O'Connell, R.M., Simmons, A.N., Matthews, S.C., 2014. Combat veterans with PTSD after mild TBI exhibit greater ERPs from posterior-medial cortical areas while appraising facial features. Journal of Affective Disorders 155, 234–240. http://dx.doi.org/10.1016/j.jad.2013.06.05724342149.

Singer, W., 1999. Neuronal synchrony: a versatile code for the definition of relations? Neuron 24, 49–65 10677026.

Smith, T.C., Ryan, M.A., Wingard, D.L., Slymen, D.J., Sallis, J.F., Kritz-Silverstein, D., 2008. New onset and persistent symptoms of post-traumatic stress disorder self reported after deployment and combat exposures: prospective population based US military cohort study. BMJ (Clinical Research Ed.) 336, 366–371. http://dx.doi.org/10.1136/bmj.39430.638241.AE18198395.

Song, T., Gaa, K., Cui, L., Feffer, L., Lee, R.R., Huang, M., 2008. Evaluation of signal space separation via simulation. Medical & Biological Engineering & Computing 46, 923–932. http://dx.doi.org/10.1007/s11517-007-0290-y18196307.

Sponheim, S.R., Clementz, B.A., Iacono, W.G., Beiser, M., 2000. Clinical and biological concomitants of resting state EEG power abnormalities in schizophrenia. Biological Psychiatry 48, 1088–1097 11094142.

Strigo, I.A., Simmons, A.N., Matthews, S.C., Grimes, E.M., Allard, C.B., Reinhardt, L.E., Paulus, M.P., Stein, M.B., 2010. Neural correlates of altered pain response in women with posttraumatic stress disorder from intimate partner violence. Biological Psychiatry 68, 442–450. http://dx.doi.org/10.1016/j.biopsych.2010.03.03420553750.

Takahashi, N., Shinomiya, S., Mori, D., Tachibana, S., 1997. Frontal midline theta rhythm in young healthy adults. Clinical EEG (Electroencephalography) 28, 49–54, 9013051.

Talairach, J., Tournoux, P., 1988. Co-planar Stereotactic Atlas of the Human BrainThieme Medical Publishers, Stuttgart and New York.

Tanielian, T., Jaycox, L.H., 2008. Invisible Wounds of War: Psychological and Cognitive Injuries, Their Consequences, and Services to Assist RecoveryRAND Corporation, Santa Monica, CA.

Tartaglione, A., Spadavecchia, L., Maculotti, M., Bandini, F., 2012. Resting state in Alzheimer's disease: a concurrent analysis of flash-visual evoked potentials and quantitative EEG. BMC Neurology 12, 145. http://dx.doi.org/10.1186/1471-2377-12-14523190493.

Taulu, S., Kajola, M., Simola, J., 2004a. Suppression of interference and artifacts by the signal space separation method. Brain Topography 16, 269–275 15379226.

Taulu, S., Simola, J., Kajola, M., 2004b. MEG recordings of DC fields using the signal space separation method (SSS). Neurology and Clinical Neurophysiology 35.

Van Veen, B.D., van Drongelen, W., Yuchtman, M., Suzuki, A., 1997. Localization of brain electrical activity via linearly constrained minimum variance spatial filtering. IEEE

Transactions on Bio-Medical Engineering 44, 867–880. http://dx.doi.org/10.1109/10.6230569282479.
Vieth, J.B., Kober, H., Grummich, P., 1996. Sources of spontaneous slow waves associated with brain lesions, localized by using the MEG. Brain Topography 8, 215–221 8728406.
Weathers, F.W., Keane, T.M., Davidson, J.R., 2001. Clinician-administered PTSD scale: a review of the first ten years of research. Depression and Anxiety 13, 132–156, 11387733.
Weathers, F.W., Litz, B.T., Herman, D.S., Huska, J.A., Keane, T.M., 1993. The PTSD checklist: reliability, validity, & diagnostic utility. Paper Presented at the Annual Meeting of the International Society for Traumatic Stress Studies.
Weathers, F.W., Ruscio, A.M., Keane, T.M., 1999. Psychometric properties of nine scoring rules for the clinician-administered posttraumatic stress disorder scale. Psychological Assessment 11, 124–133.
Whalen, P.J., Rauch, S.L., Etcoff, N.L., McInerney, S.C., Lee, M.B., Jenike, M.A., 1998. Masked presentations of emotional facial expressions modulate amygdala activity without explicit knowledge. Journal of Neuroscience: The Official Journal of the Society for Neuroscience 18, 411–418 9412517.
Whalen, P.J., Shin, L.M., McInerney, S.C., Fischer, H., Wright, C.I., Rauch, S.L., 2001. A functional MRI study of human amygdala responses to facial expressions of fear versus anger. Emotion (Washington, D.C.) 1, 70–83 12894812.
Yan, X., Brown, A.D., Lazar, M., Cressman, V.L., Henn-Haase, C., Neylan, T.C., Shalev, A., Wolkowitz, O.M., Hamilton, S.P., Yehuda, R., Sodickson, D.K., Weiner, M.W., Marmar, C.R., 2013. Spontaneous brain activity in combat related PTSD. Neuroscience Letters 547, 1–5. http://dx.doi.org/10.1016/j.neulet.2013.04.03223643995.